Iran. J. Biotechnol. July 2025;23(3): e4109 DOI: 10.30498/ijb.2025.516324.4109

Research Article

Transcriptomic Insights into Biomechanical Modulation of Gastrointestinal Function in A Rat Model of Functional Dyspepsia

Xurong Liang[1], Jiyu Yang[2], Jiyu Yang[2], Xin Wang[1], Yonggang Yang[1,*]

[1]Acupuncture and moxibustion Massage College of Changchun University of Chinese Medicine, Changchun, China
[2]Changchun Humanities and Sciences College, Changchun, China

[*]*Corresponding author*: Yonggang Yang, Acupuncture and moxibustion Massage College of Changchun University of Chinese Medicine, No. 1035 Boshuo Road, Changchun 130117, China. Tel: + 86-015792903311, Fax: +86-0431-89989333, E-mail: yonggang_yang@medicine.gz.cn

Received: 2025/04/12 ; **Accepted:** 2025/05/24

Background: Functional dyspepsia (FD) is a common gastrointestinal disorder with multifactorial etiology involving impaired motility, mucosal barrier disruption, and inflammation. Non-pharmacological biotechnological interventions, such as external biomechanical modulation, have demonstrated therapeutic benefits; however, the underlying molecular mechanisms remain largely unexplored.

Objectives: To investigate the transcriptomic and molecular changes induced by external biomechanical modulation in a rat model of FD and explore its potential as a physical biotechnological intervention for gastrointestinal dysfunction.

Materials and Methods: Thirty-six male Wistar rats were randomly assigned to control, FD model, and biomechanical modulation intervention groups. FD was induced using a multifactorial approach (tail clamping stimulation + irregular diet + ice-cold saline gavage), and external biomechanical modulation was administered daily for one week. Gastrointestinal motility was assessed by measuring gastric emptying and intestinal propulsion rates. Duodenal tissues were analyzed using transcriptome sequencing, differential gene expression profiling, Gene Ontology (GO) annotation, and Kyoto Encyclopedia of Genes and Genomes (KEGG) pathway analysis. Serum levels of TNF-α, IFN-γ, and IL-1β, as well as expression of tight junction proteins Occludin and ZO-1, were assessed via ELISA, immunofluorescence, and Western blotting.

Results: FD rats exhibited reduced motility and villus atrophy, with elevated inflammatory cytokines and downregulated tight junction proteins. Transcriptomic profiling revealed significant gene expression changes in pathways related to digestion, nutrient absorption, immune modulation, and epithelial barrier integrity. KEGG analysis highlighted the involvement of PI3K-Akt signaling, neuroactive ligand-receptor interaction, and absorption-related pathways. PI3K-Akt pathway is an important pathway to regulate cell growth, proliferation and metabolism, and plays an important regulatory role in gastrointestinal motility disorders. External biomechanical modulation reversed these alterations, improving motility, reducing inflammation, and restoring mucosal integrity. Compared with the model group, the gastric emptying rate was significantly improved, and the small intestinal propulsion rate was increased by 9%.

Conclusion: This study demonstrates that external biomechanical modulation exerts relevant effects on gastrointestinal function in FD through transcriptomic regulation of immune and barrier-related pathways. Further research should explore clinical applications and detailed mechanistic insights.

Keywords: Biomechanical modulation; Gastrointestinal biotechnology; Immune regulation Functional dyspepsia; Intestinal barrier; PI3K-Akt signaling; Transcriptomics

Copyright *© 2025 The Author(s); Published by National Institute of Genetic Engineering and Biotechnology. This is an open access article, distributed under the terms of the Creative Commons Attribution-NonCommercial 4.0 International License (http://creativecommons.org/licenses /by-nc/4.0/) which permits others to copy and redistribute material just in noncommercial usages, provided the original work is properly cited.*

1. Background

Functional dyspepsia (1) (FD) is a prevalent functional gastrointestinal disorder. To better characterize FD, the Rome IV diagnostic criteria classify it into two subtypes (2): **1)** postprandial distress syndrome (PDS), characterized by early satiety, belching, and postprandial fullness; and **2)** epigastric pain syndrome (EPS), marked by epigastric distension and burning in the upper abdomen. Traditional Chinese Medicine (TCM) literature does not explicitly mention "functional dyspepsia," but its clinical manifestations can be categorized under "fullness" and "stomach pain" (3). The pathogenesis of FD remains incompletely understood, yet its incidence and recurrence rates have risen with economic development and changes in lifestyle (4). This condition significantly impairs quality of life and imposes substantial medical and economic burdens (5-7). Current Western medical treatments primarily focus on promoting gastrointestinal moti-lity, acid suppression, and addressing anxiety and depression, with symptomatic treatment being the mainstay. However, long-term pharmacotherapy may lead to instability and increased complications (8, 9). Evidence-based medicine supports the efficacy of TCM in treating FD. Specifically, Tuina, an external therapy in TCM, has demonstrated favorable clinical outcomes in managing FD (10). Tuina exerts a bidirectional regulatory effect, enhancing gastrointestinal motility, digestion, absorption, and repairing the intestinal mucosal barrier through comprehensive multi-faceted and multi-level conditioning (11-16).

2. Objectives

In this study, we established an FD rat model to investigate the effects of external mechanical stimulation on gastrointestinal motility, duodenal mucosal status, and gene expression profiles, aiming to elucidate the biotechnological mechanisms underlying this physical intervention.

3. Materials and Methods

3.1. Laboratory Animals

Thirty-six male SPF-grade Wistar rats, weighing 200±20 g, were used in this study. The animals were provided by the Animal Center of Changchun University of Traditional Chinese Medicine under production license number SCXK (Liao) 2020-0001. The rats were housed under natural lighting conditions, with a room temperature of (25±3) °C and relative humidity of (55±5) %. They were fed standard chow and had free access to water, maintaining their natural circadian rhythm. All experimental procedures were conducted in accordance with the guidelines approved by the Animal Ethics Committee of Changchun University of Chinese Medicine (ethical review approval number: 2024306).

3.2. Reagents and Instruments

Pellet feed for rat maintenance (Changchun Yisi Laboratory Animal Technology Co., Ltd.); Electronic Balance (Sartorius, Beijing Sartorius Instrument System Co., Ltd.); Refrigerator (Haier, Qingdao Haier Co., Ltd.); Special inhalation anesthesia machine for small animals (MATRX VMR, USA); Isoflurane for veterinary use (Hebei Jindafu Pharmaceutical Co., Ltd.); Hematoxylin-eosin (HE) staining kit (Servicebio, catalog number: G1076); TNF-α, IFN-γ, IL-1β antibodies (Jianglai Biologics, catalog numbers: JL13202, JL13241, JL20884); β-actin antibody and horseradish peroxidase (HRP)-conjugated goat anti-mouse secondary antibody (Servicebio, Cat. Nos. GB15001, GB23301); Paraformaldehyde fixative solution (Biosharp, Product No.: BL539A); Thermo Scientific NanoDrop 2000 (Thermo Fisher Scientific, Waltham, MA, USA); RNA 6000 Nano kit (Agilent Technologies, catalog number: 5067-1511); NEBNext Ultra II RNA Library Prep Kit for Illumina (New England Biolabs, catalog number: E7770S); Agilent 2100 Bioanalyzer (Agilent Technologies, Santa Clara, CA, USA); Agilent High Sensitivity DNA Kit (Agilent Technologies, catalog number: 5067-4626).

3.3. Animal Grouping and Model Preparation

After a 7-day adaptive feeding period, the rats were randomly assigned to three groups (n=12 per group): the control group, the model group, and the biomechanical modulation group. Prior to the commencement of the experiment, the body weight of each rat was measured to ensure that there were no statistically significant differences in body weight among the groups.

After the completion of adaptive feeding, the FD rat model was established using a multifactorial modeling approach (17) (tail clamping stimulation + irregular diet + ice-cold saline gavage) in both the biomechanical modulation group and the model

group. Specifically, the rats' tails were clamped twice daily for 14 consecutive days. Simultaneously, the rats received ice-cold normal saline (-4 °C, 0.9% NaCl solution, 2 mL) via gavage twice daily. During this period, the rats were subjected to an irregular feeding schedule, where they had free access to food and water only every other day.

3.4. Intervention Methods

Normal group: Routine feeding without any treatment.

Biomechanical modulation group: After successful modeling, rats were anesthetized with isoflurane (4% output concentration) and subjected to abdominal rubbing for 5 minutes daily at a frequency of approximately 120 times/min, for a total of 7 sessions.

Model group: Rats received regular feeding and water after the modeling period, with no additional treatment.

3.5. Specimen Collection and Testing

3.5.1. General Condition Observation

The general condition of the rats, including mental state, coat color, and mobility, was monitored weekly. Body weight and food intake were recorded daily to assess overall health and response to treatments.

3.5.2. Gastrointestinal Motility Assessment

After a 24-hour fasting period, six rats from each group were randomly selected and gavaged with a semi-solid milk paste containing activated carbon powder (prepared by mixing 5 g of sodium carboxymethyl cellulose, 8 g of milk powder, 4 g of sugar, 4 g of starch, and 2 g of activated carbon powder in 125 mL of distilled water). Thirty minutes post-gavage, rats were anesthetized using an inhalation anesthesia machine, and the entire gastrointestinal tract was removed after laparotomy. Gastric emptying rate was calculated as follows:

Gastric emptying rate=
(Weight of gastric residue)/(Weight of administered semi-solid milk paste)×100%

The small intestine propulsion rate was measured by flattening the small intestine on white paper and calculating the distance from the pylorus to the leading edge of the black semi-solid paste relative to the total length from the pylorus to the ileocecal junction:

Small intestine propulsion rate=
(Distance from pylorus to leading edge of paste)/(Total length from pylorus to ileocecal junction)×100%

3.6. Histopathological Analysis by HE Staining

The remaining six rats from each group were anesthetized and subjected to laparotomy for blood collection from the abdominal aorta. Duodenal tissues were harvested, rinsed with pre-chilled normal saline, and fixed in 4% paraformaldehyde solution. Tissues were then dehydrated, embedded in paraffin, sectioned at 5 μm thickness, and stained with hematoxylin and eosin (HE) for histopathological evaluation under light microscopy.

3.7. Transcriptome Sequencing

Half of the harvested duodenal tissues were fixed in RNAlater solution at room temperature for 24 hours and stored at -80 °C for subsequent RNA extraction. Total RNA was extracted using a commercial kit, and RNA integrity was verified by agarose gel electrophoresis. mRNA was purified based on its polyA tail, fragmented, and reverse-transcribed into cDNA. The resulting cDNA was used to construct sequencing libraries, which were sequenced using the Illumina platform. Differential gene expression analysis was performed using the R package, with genes showing fold changes >2 or <0.5 and $P < 0.05$ considered differentially expressed. Gene ontology (GO) and Kyoto Encyclopedia of Genes and Genomes (KEGG) pathway enrichment analyses were conducted to elucidate the biological functions and pathways associated with the differentially expressed genes.

3.8. ELISA for Inflammatory Cytokines

Serum levels of TNF-α, IFN-γ, and IL-1β were measured using commercially available ELISA kits according to the manufacturer's instructions. Briefly, samples were placed on ice and stabilized at 4 °C, while the ELISA kit was brought to room temperature and thoroughly mixed. Standards were prepared, and samples were added to the microplate for incubation at room temperature for 1 hour. After washing, enzyme-conjugated reagents were added for incubation, followed by a colorimetric reaction and stop solution addition. The concentration of each cytokine was determined by linear regression analysis of the optical density (OD) values, and the actual concentration was

calculated by multiplying with the dilution factor.

3.9. Immunofluorescence for Tight Junction Proteins

Duodenal tissue sections were deparaffinized, re-hydrated, and subjected to antigen retrieval in high-temperature repair solution. Sections were then washed with PBS, blocked with BSA, and incubated overnight at 4 °C with primary antibodies against occludin and ZO-1. After washing, sections were incubated with secondary antibodies for 2 hours at room temperature, followed by nuclear staining with DAPI. Fluorescence images were captured under a fluorescence microscope to assess the expression and distribution of tight junction proteins.

3.10. Western Blot Analysis

Total protein was extracted from duodenal tissues using a lysis buffer containing protease inhibitors. Protein concentration was measured using a BCA kit. Equal amounts of protein were separated by SDS-PAGE and transferred to PVDF membranes. Membranes were blocked with 5% skimmed milk powder for 1-2 hours, followed by incubation with primary antibodies against occludin, ZO-1, and β-actin (as a loading control) overnight at 4 °C. After washing, membranes were incubated with HRP-conjugated secondary antibodies for 1 hour at room temperature. Specific protein bands were visualized using chemiluminescence, and band intensities were quantified using ImageJ software.

3.11. Statistical Analysis

Dates were analyzed using SPSS 26.0 software. Continuous data are presented as mean ± SD. One-way ANOVA was used for comparisons among groups, followed by LSD tests for pairwise comparisons. $P < 0.05$ was considered statistically significant.

4. Results

4.1. General Condition and Gastric Tissue Morphology

4.1.1. General Condition, Body Weight, and Food Intake

Rats in the normal group exhibited smooth and bright fur, good mental state, and normal feces. In contrast, the model group showed dull coat color, decreased emotional responsiveness, emaciation, and thin feces with a sour odor. The biomechanical modulation group exhibited improved coat smoothness and emotional response, with feces returning to normal. Compared to the normal group, the model group had

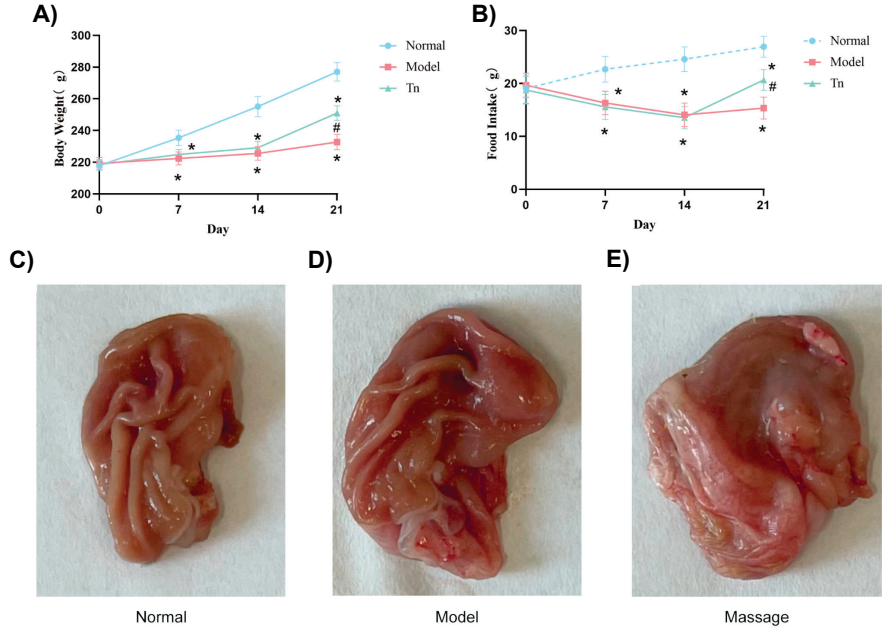


Figure 1. General Condition and Gastric Tissue Morphology. **A-B**) Changes in body weight **A**) and food intake **B**) of rats in the three groups. **C-E**) Comparison of the gross morphology of gastric tissue in normal group **C**), model group **D**) and massage group **E**). Tn, massage group.

significantly reduced body weight and food intake ($P < 0.01$; **Fig. 1A-1B**). The biomechanical modulation group showed significant increases in body weight and food intake compared to the model group ($P < 0.01$; **Fig. 1A-1B**).

4.1.2. Gastric Tissue Morphology

The gastric mucosa of the normal group appeared smooth and pale pink (**Fig. 1C-1D**). The model group showed no obvious lesions, while the biomechanical modulation group was similar to the normal group.

4.2. Gastrointestinal Motility

The gastric emptying rate and small intestine propulsion rate were significantly lower in the model group compared to the normal group ($P < 0.01$; **Table 1**, **Fig. 2A-2B**). The biomechanical modulation group exhibited significant improvements in both parameters compared to the model group ($P < 0.01$; **Table 1**, **Fig. 2A-2B**).

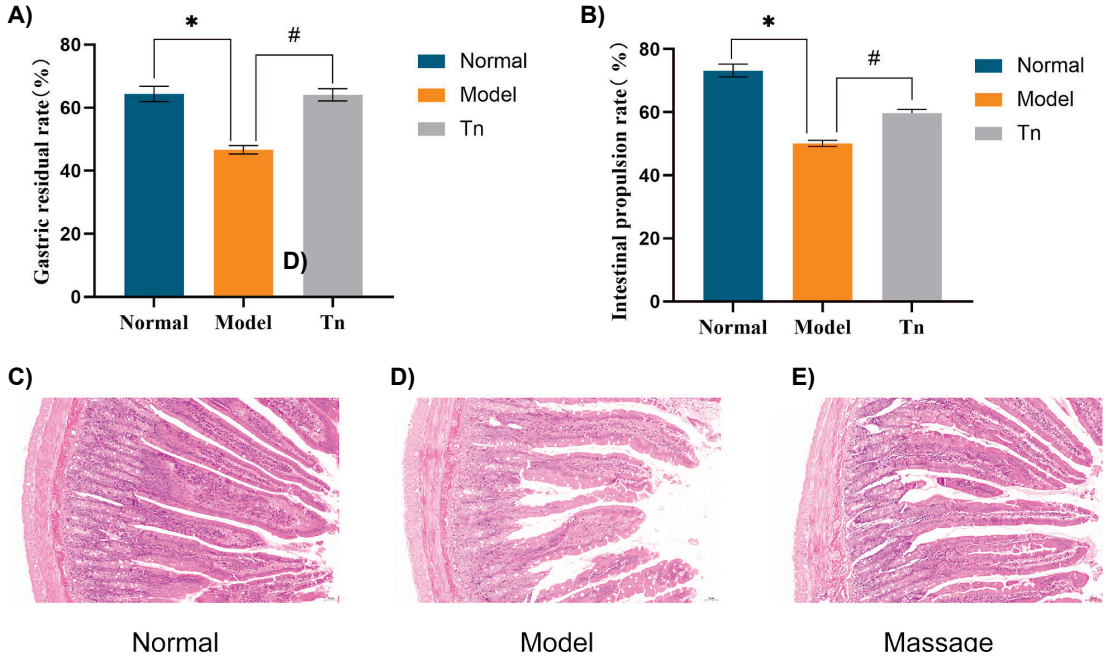


Figure 2. Gastrointestinal Motility and Duodenal Histopathology. **A-B**) Changes in gastric emptying rate **A**) and small intestinal propulsion rate **B**) in three groups of rats. **C-E**) HE staining of duodenum in normal **C**), model **D**), massage **E**) groups of rats. Tn, massage group.

Table 1. Comparison of gastric emptying rate and small intestinal propulsion rate among three groups of rats (x ± s)

Group	N	Gastric emptying rate (%)	Small intestine propulsion rate (%)
Normal	6	64.38±2.42	73.18±2.05
Model	6	46.67±1.33*	50.11±0.97*
Tn	6	64.10±1.94#	59.72±1.18#

Note: After treatment, compared with the normal group, * P<0.01; Compared with the model group, # P<0.01.

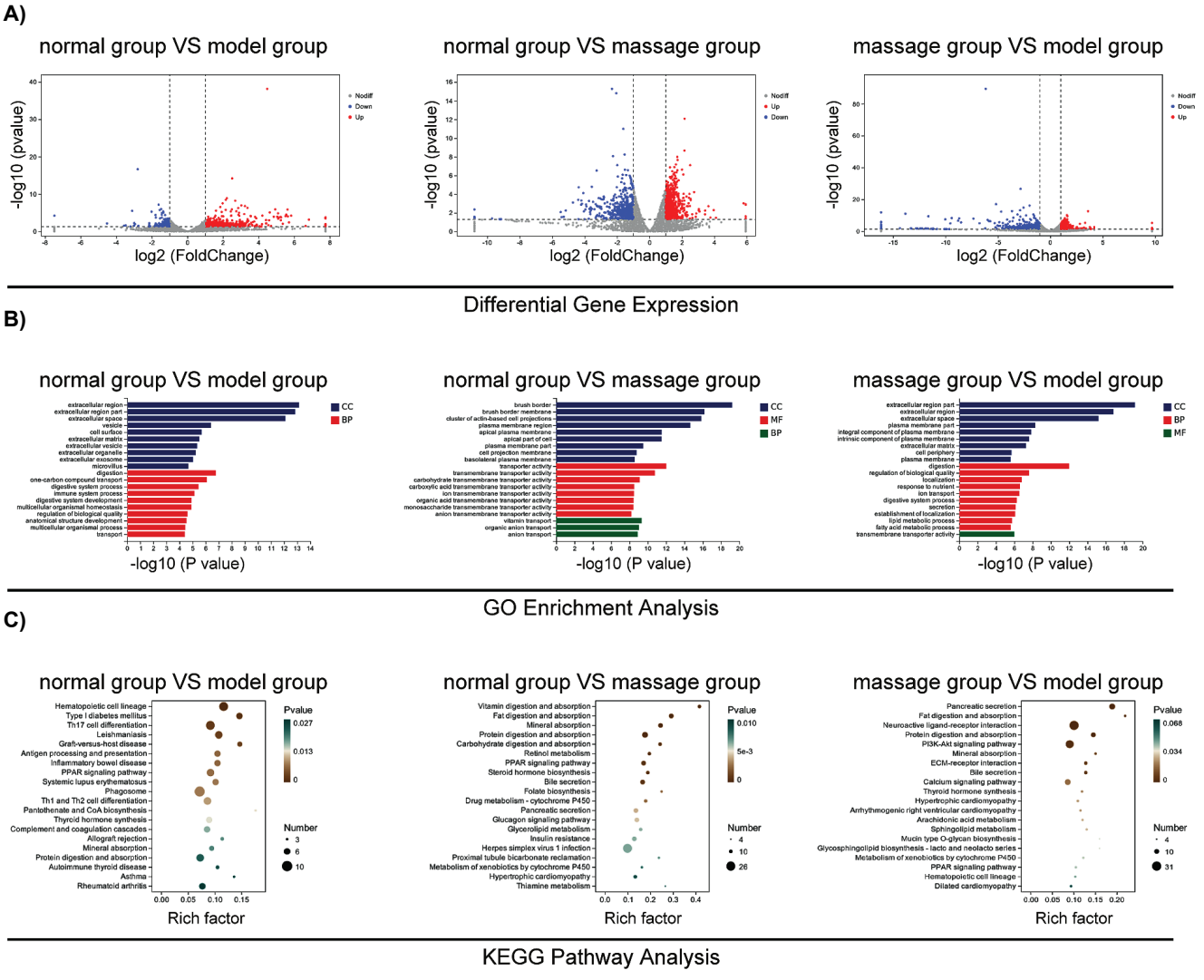


Figure 3. Differential Gene Expression and Functional Analysis. **A**) Volcano plots illustrating differential gene expression between groups. The x-axis represents the log2 fold change, and the y-axis represents the negative log10 of the adjusted p-value. Red dots indicate upregulated genes, blue dots indicate downregulated genes, and grey dots represent genes without significant changes. The plots compare the normal group versus the model group, the normal group versus the massage group, and the massage group versus the model group. **B**) Gene Ontology (GO) enrichment analysis of differentially expressed genes. The bar graphs show the -log10 of the p-value on the x-axis and the number of genes associated with each GO term on the y-axis. The terms are categorized into three main GO domains: Biological Process (BP), Cellular Component (CC), and Molecular Function (MF), represented by different colors. **C**) Kyoto Encyclopedia of Genes and Genomes (KEGG) pathway analysis of differentially expressed genes. The bubble charts display the pathways with significant enrichment. The x-axis represents the rich factor, indicating the ratio of the number of differentially expressed genes to the total number of genes in the pathway, while the y-axis shows the -log10 of the p-value. The size of the bubbles corresponds to the number of genes involved in each pathway.

4.3. Histopathological Observations of Duodenum

The duodenal mucosa of the normal group was intact with neatly arranged villi (**Fig. 3C**). The model group showed disordered villi arrangement, with some villi lodging, fusing, and falling off (**Fig. 3D**). The biomechanical modulation group exhibited relatively intact mucosa with neatly arranged villi (**Fig. 3E**).

4.4. Transcriptomic Analysis

4.4.1. Differential Gene Expression

Differentially expressed genes were identified using the criteria $|log2FC| \geq 1$ and $P < 0.05$. Genes meeting these criteria were classified as differentially expressed. Sequencing results revealed that, compared to the normal group, the model group exhibited a total of 566 significantly differentially expressed genes, comprising 430 up-regulated and 136 down-regulated genes (**Fig. 3A** left). The top 10 genes are listed in **Table 2**. When comparing the biomechanical modulation group with the model group, a total of 1012 significantly differentially expressed genes were identified, including 437 up-regulated and 575 down-regulated genes (**Fig. 3A** right). The top 10 genes are presented in **Table 3**. Relative to the normal group, the biomechanical modulation group showed a total of 1140 significantly differentially expressed genes, consisting of 653 up-regulated and 487 down-regulated genes (**Fig. 3A** middle). The top 10 genes are detailed in **Table 4**. Additionally, three groups of differentially expressed genes were analyzed, yielding a total of four common genes with IDs ENSRNOG00000013973, ENSRNOG00000019467, ENSRNOG0000000841, and ENSRNOG00000064941.

4.4.2. GO Enrichment Analysis

Gene ontology (GO) enrichment analysis was performed to categorize the biological processes, cellular

Table 2. Genes with Significant Differences between the Model Group and the normal Group (Top 10)

Gene id	Gene name	log2(fc)	pval	padj	regulation
ENSRNOG00000014740	Gast	4.483515	7.23E-39	1.335E-34	Up
ENSRNOG00000054142	Slc30a2	-2.7968	2.23E-17	2.06E-13	Down
ENSRNOG00000017712	Cartpt	2.515592	6.58E-15	4.049E-11	Up
ENSRNOG00000025384	Slc2a10	2.216103	1.26E-09	5.801E-06	Up
ENSRNOG00000021027	Dbp	2.158366	3.33E-09	1.231E-05	Up
ENSRNOG00000020245	Syt8	2.686454	5.97E-09	1.836E-05	Up
ENSRNOG00000000525	Pi16	1.9785	2.9E-08	7.633E-05	Up
ENSRNOG00000000451	RT1-Ba	-1.62376	6.81E-08	0.0001572	Down
ENSRNOG00000014021	Matn4	3.032351	1.03E-07	0.0002108	Up
ENSRNOG00000056001	Sftpd	3.233558	1.66E-07	0.000307	Up

Table 3. Genes with Significant Differences between the Tuina Group and the Model Group (Top 10)

Gene id	Gene name	log2(fc)	pval	padj	regulation
ENSRNOG00000014740	Gast	-6.1618	3.35E-90	6.24E-86	Down
ENSRNOG00000017712	Cartpt	-2.83234	2.55E-27	2.37E-23	Down
ENSRNOG00000015306	Slc9a4	-5.18297	1.12E-17	6.94E-14	Down
ENSRNOG00000009629	Car2	-1.97059	7.21E-17	3.35E-13	Down
ENSRNOG00000011907	Krt23	-2.55851	1.38E-15	5.14E-12	Down
ENSRNOG00000000542	Dnah8	-2.87312	6.16E-14	1.91E-10	Down
ENSRNOG00000033209	Bmp8b	-3.65124	1.83E-13	4.88E-10	Down
ENSRNOG00000065115	-	3.603833	2.23E-13	5.18E-10	Up
ENSRNOG00000056001	Sftpd	-4.67573	4.52E-13	9.35E-10	Down
ENSRNOG00000008838	Gkn1	-16.1454	1.29E-12	2.40E-09	Down

components, and molecular functions associated with the differentially expressed genes in each comparison group. The analysis revealed distinct patterns of enrichment across the three groups.

4.4.2.1. Comparison of Model Group vs. Normal Group:

A total of 972 differentially expressed genes were identified between the model group and the normal group. These genes were significantly enriched in 82 GO terms related to cellular components, primarily including extracellular regions (e.g., extracellular space, extracellular matrix, and microvilli). Molecular function annotations highlighted 180 terms, with a focus on transporter activities (e.g., one-carbon compound transport, transmembrane transporter activity) and immune system processes. Biological processes were dominated by digestion-related terms, with 710 annotations (**Fig. 3B** left). These findings suggest that the development of functional dyspepsia in the model group is associated with significant alterations in extracellular components and immune-related functions, as well as impaired digestive processes.

4.4.2.2. Comparison of Biomechanical Modulation Group vs. Normal Group:

In the biomechanical modulation group compared to the normal group, 1431 differentially expressed genes were enriched in 132 GO terms related to cellular components, including brush border, brush border membrane, and actin-based cell projections. Molecular functions were characterized by 257 annotations, with a focus on transporter activities (e.g., protein transporter activity, carbohydrate transmembrane trans-porter activity). Biological processes were enriched in 1042 terms, highlighting pathways related to nutrient transport (e.g., vitamin transport, organic anion transport) and digestive processes (**Fig. 3B** middle). These results indicate that abdominal rubbing induces significant changes in cellular components and molecular functions associated with nutrient absorption and digestion.

4.4.2.3. Comparison of Biomechanical Modulation Group vs. Model Group:

When comparing the biomechanical modulation group to the model group, 1654 differentially expressed genes were identified. These genes were enriched in 158 GO terms related to cellular components, such as extracellular regions and plasma membrane components. Molecular functions included 267 annotations, with a focus on transmembrane transporter activities (e.g., inorganic molecular entity transmembrane transporter activity). Biological processes were dominated by 1229 annotations, highlighting pathways related to digestion, ion transport, and localization responses to

Table 4. Genes with Significant Differences between Massage Group and normal Group (Top 10)

Gene id	Gene name	log2(fc)	pval	padj	regulation
ENSRNOG00000028889	Slc51b	-2.31662	5.29E-16	9.81E-12	Down
ENSRNOG00000054142	Slc30a2	-2.04751	1.56E-15	1.45E-11	Down
ENSRNOG00000012067	Fam111a	2.163638	8.16E-13	5.05E-09	Up
ENSRNOG00000001765	Slc51a	-1.61623	1.03E-11	4.77E-08	Down
ENSRNOG00000004667	Gen1	2.154069	2.16E-09	8.01E-06	Up
ENSRNOG00000022054	Paqr7	-1.53319	5.73E-09	1.77E-05	Down
ENSRNOG00000065254	RT1-CE16	-2.25249	8.54E-09	2.26E-05	Down
ENSRNOG00000015921	Esco2	1.707711	1.03E-08	2.39E-05	Up
ENSRNOG00000009503	Depdc1	1.733627	2.22E-08	4.57E-05	Up
ENSRNOG00000046968	Nol8	1.625541	6.61E-08	0.00012264	Up

nutrients (**Fig. 3B** right). These findings suggest that abdominal rubbing not only restores normal digestive processes but also modulates cellular components and molecular functions to counteract the pathological changes observed in the model group.

Overall, the GO enrichment analysis provides a compre-hensive overview of the biological processes, cellular components, and molecular functions affected by functional dyspepsia and the therapeutic intervention of abdominal rubbing. These results highlight the multifaceted nature of the disease and the broad regulatory effects of biomechanical modulation therapy.

4.4.3. KEGG Pathway Analysis

Kyoto Encyclopedia of Genes and Genomes (KEGG) pathway analysis was conducted to elucidate the metabolic and signaling pathways associated with the differentially expressed genes. The analysis revealed distinct pathway enrichments across the three groups.

4.4.3.1. Comparison of Model Group vs. Normal Group:

The model group exhibited significant enrichment in 29 pathways compared to the normal group. The top five pathways included Hematopoietic cell lineage, Type I diabetes mellitus, Th17 cell differentiation, Leishmaniasis, and Herpes simplex virus host interactions (**Fig. 3C** left). These pathways are primarily associated with immune response and inflammation, suggesting that the development of functional dyspepsia in the model group is characterized by significant immune dysregulation and inflammatory processes.

4.4.3.2. Comparison of Biomechanical Modulation Group vs. Normal Group:

In the biomechanical modulation group compared to the normal group, 39 pathways were significantly enriched. The top five pathways included Vitamin digestion and absorption, Fat digestion and absorption, Mineral absorption, Protein digestion and absorption, and Carbohydrate digestion and absorption (**Fig. 3C** middle). These findings indicate that abdominal rubbing induces significant changes in pathways related to nutrient digestion and absorption, highlighting its potential therapeutic effects on gastrointestinal function.

4.4.3.3. Comparison of Biomechanical Modulation Group vs. Model Group:

When comparing the biomechanical modulation group to the model group, 19 pathways were significantly enriched. The top five pathways included Pancreatic secretion, Fat digestion and absorption, Neuroactive ligand-receptor interaction, Protein digestion and absorption, and PI3K-Akt signaling pathway (**Fig. 3C** right). The PI3K-Akt pathway is a critical regulator of cell growth, survival, and metabolism, and its involvement suggests that abdominal rubbing may exert its therapeutic effects by modulating this pathway. Additionally, the enrichment of pathways related to pancreatic secretion and neuroactive ligand-receptor interactions indicates that abdominal rubbing may influence gastrointestinal motility and neurotransmitter signaling.

In summary, the KEGG pathway analysis provides insights into the metabolic and signaling pathways affected by functional dyspepsia and the therapeutic intervention of abdominal rubbing. These findings highlight the potential mechanisms underlying the therapeutic effects of biomechanical modulation therapy, including modulation of immune responses, enhancement of digestive processes, and regulation of key signaling pathways.

4.5. Inflammatory Factors and Tight Junction Proteins

4.5.1. Inflammatory Factors

Serum levels of TNF-α, IFN-γ, and IL-1β were significantly elevated in the model group compared to the normal group ($P < 0.01$; **Fig. 4A-C**). The biomechanical modulation group showed significant reductions in these inflammatory factors compared to the model group ($P < 0.01$; **Fig. 4A-C**).

4.5.2. Tight Junction Proteins

Immunofluorescence and WB analyses revealed decreased expression of occludin and ZO-1 in the model group compared to the normal group ($P < 0.01$; **Fig. 4D-4H**). The biomechanical modulation group exhibited restored expression of these tight junction proteins compared to the model group ($P < 0.01$; **Fig. 4, Fig. 4D-4H**).

5. Discussion

Functional dyspepsia (FD) is a complex disorder with

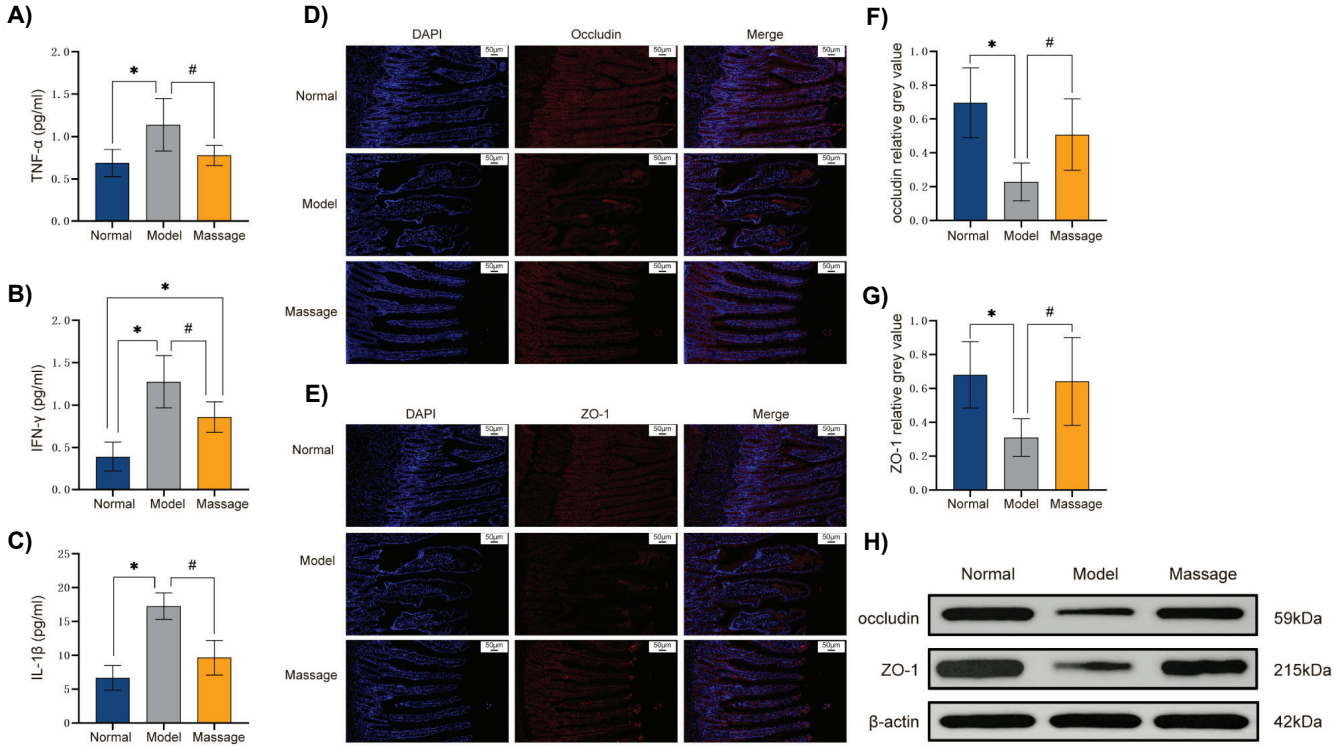


Figure 4. Inflammatory Factors and Tight Junction Proteins. **A**) Changes in serum TNF-α levels in the three groups.Bar chart showing the serum levels of TNF-α in normal, model, and massage groups. The model group exhibited significantly higher levels compared to the normal group, while the massage group showed a significant reduction. **B**) Changes in serum IFN-γ levels in the three groups. Bar chart showing the serum levels of IFN-γ in normal, model, and massage groups. Similar to TNF-α, the model group had elevated levels, which were reduced in the massage group. **C**) Changes in serum IL-1β levels in the three groups. Bar chart showing the serum levels of IL-1β in normal, model, and massage groups. The model group had increased levels, which were decreased in the massage group. **D**) Immunofluorescence detection of Occludin in duodenal tissue. Fluorescence microscopy images showing the expression of occludin (red) in duodenal tissues, with nuclei stained with DAPI (blue). The model group showed reduced expression, while the massage group exhibited restored expression. Scale bar, 50 μm. **E**) Immunofluorescence detection of ZO-1 in duodenal tissue. Fluorescence microscopy images showing the expression of ZO-1 (red) in duodenal tissues, with nuclei stained with DAPI (blue). The model group had decreased expression, which was increased in the massage group. Scale bar, 50 μm. **F**) Quantification of Occludin protein expression (Western Blot). Bar chart showing the relative expression levels of occludin in duodenal tissues, as determined by Western blot analysis. The model group had reduced expression, which was increased in the massage group. **G**) Quantification of ZO-1 protein expression (Western Blot). Bar chart showing the relative expression levels of ZO-1 in duodenal tissues, as determined by Western blot analysis. The model group had decreased expression, which was increased in the massage group. **H**) Western Blot analysis of occludin and ZO-1. Western blot images showing the protein bands for occludin and ZO-1 in duodenal tissues, with β-actin as a loading control. The model group exhibited reduced bands, while the massage group showed restored expression.

unclear pathogenesis, often characterized by recurrent symptoms that significantly impact quality of life. Current treatments for FD are limited in efficacy and may cause side effects. Traditional Chinese Medicine (TCM), particularly Tuina (biomechanical modulation), has shown promise in treating FD by regulating gastrointestinal motility, reducing inflammation, and repairing the intestinal mucosal barrier. This study aimed to elucidate the molecular mechanisms underlying the therapeutic effects of abdominal rubbing in a rat model of FD.

Our results demonstrated that abdominal rubbing

significantly improved the general condition of FD model rats, as evidenced by increased body weight and food intake (**Fig. 1A-B**). This improvement was accompanied by enhanced gastrointestinal motility, with significant increases in gastric emptying rate and small intestine propulsion rate compared to the model group (**Table 1, Fig. 2A-2B**). Histopathological analysis revealed that the duodenal mucosa of the biomechanical modulation group was relatively intact, with neatly arranged villi, similar to the normal group (**Fig. 2C-2E**).

Transcriptomic analysis provided insights into the molecular mechanisms underlying the therapeutic effects of abdominal rubbing. Compared to the normal group, the model group exhibited significant changes in gene expression profiles, with enrichment in pathways related to immune response and digestion (**Fig. 3B**). The biomechanical modulation group showed enrichment in pathways related to digestion, absorption, and ion transport, as well as the PI3K-Akt signaling pathway (**Fig. 3B**). The PI3K-Akt pathway is known to regulate cell growth, proliferation, and metabolism, and its dysregulation has been implicated in gastrointestinal motility disorders (18-20). Our findings suggest that abdominal rubbing may exert its therapeutic effects by modulating this pathway.

Inflammatory cytokines play a crucial role in the pathogenesis of FD (21,22). Our study showed that the model group had significantly elevated levels of TNF-α, IFN-γ, and IL-1β compared to the normal group (**Fig. 4A-C**). Abdominal rubbing significantly reduced the expression of these inflammatory factors, indicating its anti-inflammatory effects (23). This reduction in inflammation may contribute to the normalization of gastrointestinal motility and the repair of the intestinal mucosal barrier.

The integrity of the intestinal mucosal barrier is essential for maintaining gastrointestinal health. Our study demonstrated that the model group had decreased expression of tight junction proteins occludin and ZO-1, as shown by immunofluorescence and WB analyses (**Fig. 4D-H**). The biomechanical modulation group exhibited restored expression of these proteins, suggesting that abdominal rubbing promotes the repair of the intestinal mucosal barrier (24,25). This finding is consistent with previous studies showing that biomechanical modulation can enhance tight junction protein expression and reduce intestinal permeability (24,26).

This study has several limitations that should be considered. First, the study was conducted in a rat model, and the findings may not directly translate to humans due to species differences in gastrointestinal physiology and disease mechanisms. Second, the study focused on a short-term intervention and did not evaluate the long-term effects of abdominal rubbing on FD. Third, the molecular mechanisms underlying the therapeutic effects of abdominal rubbing were explored through transcriptomic analysis, but further studies are needed to validate the key signaling pathways and targets identified. Lastly, the study did not investigate potential non-genetic factors that could contribute to the therapeutic effects of abdominal rubbing, such as changes in gut microbiota or neuroendocrine responses.

This study demonstrates that external mechanical stimulation, as a biotechnological physical intervention, can effectively modulate gastrointestinal function and restore mucosal integrity in a rat model of FD. The use of high-throughput transcriptomic analysis allowed for the identification of key molecular pathways, such as PI3K-Akt signaling, that are responsive to biomechanical cues. These findings are consistent with emerging trends in gut bioengineering, where mechanical forces are harnessed to regulate tissue homeostasis, promote regeneration, and develop innovative therapeutic strategies. The integration of mechanical stimulation protocols with other biotechnological platforms, such as organ-on-chip systems and targeted drug delivery, holds promise for the development of next-generation therapies for gastrointestinal disorders.

In summary, this study provides evidence that abdominal rubbing improves gastrointestinal motility and repairs the intestinal mucosal barrier in FD model rats. These therapeutic effects are likely mediated through the modulation of inflammatory responses and the activation of key signaling pathways, such as PI3K-Akt. Future studies should further validate these findings using techniques such as RT-PCR and WB to confirm the involvement of key signaling pathways and targets. Additionally, clinical trials are warranted to explore the therapeutic potential of abdominal rubbing in patients with FD.

Conflict of Interests

The authors declared no conflict of interest.

Funding
This study did not receive any funding in any form.

Authors' contributions
XL and YY designed the study and performed the experiments, JY and JY collected the data, JY, JY and XW analyzed the data, XL and YY prepared the manuscript. All authors read and approved the final manuscript.

References
1. Talley NJ, Ford AC. Functional Dyspepsia. *New Engl J Med*. 2015;**373**(19):1853-1863. doi: 10.1056/NEJMra1501505.
2. Enck P, Azpiroz F, Boeckxstaens G, Elsenbruch S, Feinle-Bisset C, Holtmann G, *et al*. Functional dyspepsia. *Nat Rev Dis Primers*. 2017;**3**(1):1-20. doi: 10.1038/nrdp.2017.81.
3. Ford AC, Mahadeva S, Carbone MF, Lacy BE, Talley NJ. Functional dyspepsia. *Lancet*. 2020;**396**(10263):1689-1702. doi: 10.1016/S0140-6736(20)30469-4.
4. Talley NJ, Holtmann G, Walker MM. Therapeutic strategies for functional dyspepsia and irritable bowel syndrome based on pathophysiology. *J Gastroenterol*. 2015;**50**(6):601-613. doi: 10.1007/s00535-015-1076-x.
5. Tolba R, Shroll J, Kanu A, Rizk MK. The Epidemiology of Chronic Abdominal Pain. *Springer New York*. 2015;
6. Kovacs DB, Szekely A, Hubai AG, Palsson O. Prevalence, epidemiology and associated healthcare burden of Rome IV irritable bowel syndrome and functional dyspepsia in the adult population of Gibraltar. *Bmj Open Gastroenter*. 2022;**9**(1) doi: 10.1136/bmjgast-2022-000979.
7. Yang YJ, Bang CS, Baik GH, Park TY, Shin SP, Suk KT, *et al*. Prokinetics for the treatment of functional dyspepsia: Bayesian network meta-analysis. *Bmc Gastroenterol*. 2017;**17**(1):83. doi: 10.1186/s12876-017-0639-0.
8. Camilleri M, Bharucha AE, Farrugia G. Epidemiology, mechanisms, and management of diabetic gastroparesis. *Clin Gastroenterol H*. 2011;**9**(1):5-12, quiz e7. doi: 10.1016/j.cgh.2010.09.022.
9. Ho L, Zhong C, Wong C, Wu J, Chan K, Wu I, *et al*. Chinese herbal medicine for functional dyspepsia: a network meta-analysis of prokinetic-controlled randomised trials. *Chin Med-Uk*. 2021;**16**(1):140. doi: 10.1186/s13020-021-00556-6.
10. Dai N, He Q, Liu X, Fang M, Xiong M, Li X, *et al*. Therapeutic massage/Tuina for treatment of functional dyspepsia: a systematic review and meta-analysis of randomized controlled trials. *Qual Life Res*. 2023;**32**(3):653-667. doi: 10.1007/s11136-022-03228-6.
11. Yuan Q, Wang X, Zhou L, Li C, Lu Q, Wang H, *et al*. Abdominal massage for chronic constipation in the elderly: a systematic review and meta-analysis protocol. *Bmj Open*. 2024;**14**(1):e074780. doi: 10.1136/bmjopen-2023-074780.
12. Liang SB, Lai BY, Cao HJ, Cai QH, Bai X, Li J, *et al*. Pediatric tuina for the treatment of anorexia in children under 14 years: a systematic review and meta-analysis of randomized controlled trials. *Complement Ther Med*. 2020;**51**:102411. doi: 10.1016/j.ctim.2020.102411.
13. Bu FL, Han M, Lu CL, Liu XH, Wang WG, Lai JL, *et al*. A systematic review of Tuina for irritable bowel syndrome: Recommendations for future trials. *Complement Ther Med*. 2020;**52**:102504. doi: 10.1016/j.ctim.2020.102504.
14. Wang H, Liu Z, Yu T, Zhang Y, Jiao Y, Wang X, *et al*. The effect of tuina on ulcerative colitis model mice analyzed by gut microbiota and proteomics. *Front Microbiol*. 2022;**13**:976239. doi: 10.3389/fmicb.2022.976239.
15. Dehghan M, Malakoutikhah A, Ghaedi HF, Zakeri MA. The Effect of Abdominal Massage on Gastrointestinal Functions: a Systematic Review. *Complement Ther Med*. 2020;**54**:102553. doi: 10.1016/j.ctim.2020.102553.
16. Fang YP, Huang YT, Chen D, Kan Y, Wang JW, Kang XL, *et al*. [Systematic review and Meta analysis on the effectiveness and safety of tuina in treatment of functional constipation]. *Zhongguo Zhen Jiu*. 2021;**41**(6):691-698. doi: 10.13703/j.0255-2930.20200411-0004.
17. Xiao Z, Xu J, Tan J, Zhang S, Wang N, Wang R, *et al*. Zhizhu Kuanzhong, a traditional Chinese medicine, alleviates gastric hypersensitivity and motor dysfunction on a rat model of functional dyspepsia. *Front Pharmacol*. 2022;**13**:1026660. doi: 10.3389/fphar.2022.1026660.
18. Ma P, Gu B, Xiong W, Tan B, Geng W, Li J, *et al*. Glimepiride promotes osteogenic differentiation in rat osteoblasts via the PI3K/Akt/eNOS pathway in a high glucose microenvironment. *Plos One*. 2014;**9**(11):e112243. doi: 10.1371/journal.pone.0112243.
19. Li P, Huang D, Gu X. Exploring the dual role of circRNA and PI3K/AKT pathway in tumors of the digestive system. *Biomed Pharmacother*. 2023;**168**:115694. doi: 10.1016/j.biopha.2023.115694.
20. Su WY, Tian LY, Guo LP, Huang LQ, Gao WY. PI3K signaling-regulated metabolic reprogramming: From mechanism to application. *Bba-Rev Cancer*. 2023;**1878**(5):188952. doi: 10.1016/j.bbcan.2023.188952.
21. Li L, Fu M, Chen F, Ji H, Zhou G, Chen L, *et al*. The mediating effect of circulating inflammatory proteins on the relationship between gut microbiota and FD: a bidirectional Mendelian randomization study. *Sci Rep-Uk*. 2024;**14**(1):23785. doi: 10.1038/s41598-024-74717-6.
22. Longstreth GF. Functional Dyspepsia. *New Engl J Med*. 2016;**374**(9):895. doi: 10.1056/NEJMc1515497.
23. Wang Q, Lin J, Yang P, Liang Y, Lu D, Wang K, *et al*. Effect of Massage on the TLR4 Signalling Pathway in Rats with Neuropathic Pain. *Pain Res Manag*. 2020;**2020**:8309745. doi: 10.1155/2020/8309745.
24. Zhang W, Li H, Zhao N, Luo X, Liu S, Bao A, *et al*. Lactobacillus johnsonii BS15 combined with abdominal massage on intestinal permeability in rats with nonalcoholic fatty liver and cell biofilm repair. *Bioengineered*. 2021;**12**(1):6354-6363. doi: 10.1080/21655979.2021.1954134.
25. Matar A, Damianos JA, Jencks KJ, Camilleri M. Intestinal Barrier Impairment, Preservation, and Repair: An Update. *Nutrients*. 2024;**16**(20) doi: 10.3390/nu16203494.
26. Huang Y, Ma Q, He J, Liang X, Mai Q, Luo H, *et al*. Abdominal massage alleviates functional diarrhea in immature rats via modulation of intestinal microbiota and tight junction protein. *Front Pediatr*. 2022;**10**:922799. doi: 10.3389/fped.2022.922799.